

Exploring probability distributions for bivariate temporal granularities

Abstract

Recent advances in technology greatly facilitates recording and storing data at much finer temporal scales than was previously possible. As the frequency of time-oriented data increases, the number of questions about the observed variable that need to be addressed by visual representation also increases. We propose some new tools to explore this type of data, which deconstruct time in many different ways. There are several classes of time deconstructions including linear time granularities, circular time granularities and aperiodic calendar categorizations. Linear time granularities respect the linear progression of time such as hours, days, weeks and months. Circular time granularities accommodate periodicities in time such as hour of the day, and day of the week. Aperiodic calendar categorizations are neither linear nor circular, such as day of the month or public holidays.

The hierarchical structure of linear granularities creates a natural nested ordering resulting in single-order-up and multiple-order-up granularities. For example, hour of the week and second of the hour are both multiple-order-up, while hour of the day and second of the minute are single-order-up.

Visualizing data across granularities which are either single-order-up or multiple-order-up or periodic/aperiodic helps us to understand periodicities, pattern and anomalies in the data. Because of the large volume of data available, using displays of probability distributions conditional on one or more granularities is a potentially useful approach. This work provides tools for creating granularities and exploring the associated time series within the tidy workflow, so that probability distributions can be examined using the range of graphics available in ggplot2(Wickham 2016).

Contents

1	Introduction	2
2	Linear Time granularities	3
2.1	Definitions and Relationships	3
2.2	Computation through Calendar Algebra	5
3	Cyclic Time granularities	6
3.1	Circular	6
3.2	Quasi-circular	7
3.3	Aperiodic	10
4	Computing cyclic time granularities	11
4.1	Multiple-order from single-order	11
4.2	Single-order from multiple-order	12
5	Data structure	13
5.1	Synergy of the cyclic granularities	14
5.2	Density estimation of measured variable	14
6	Visualization	15
6.1	Choice of Plots	15
6.2	Effect of synergy of time granularities	17
6.3	Effect of number of observations	17
7	Applications	19
7.1	Smart meter data of Australia	19
7.2	T20 cricket data of Indian Premiere League	26
8	Discussion	28

1 Introduction

Temporal data are available at various resolutions depending on the context. Social and economic data like GDP is often collected and reported at coarse temporal scales like monthly, quarterly or annually. With recent advancement in technology, more and more data are recorded at much finer temporal scales. Energy consumption is collected every half an hour, while energy supply is collected every minute and web search data might be recorded every second. As the frequency of data increases, the number of questions about the periodicity of the observed variable also increases. For example, data collected at an hourly scale can be analyzed using coarser temporal scales like days, months or quarters. This approach requires deconstructing time in various possible ways called time granularities (Aigner et al. 2011). It is important to be able to navigate through all of these temporal granularities to have multiple perspectives on the periodicity of the observed data. This idea aligns with the notion of EDA (Tukey 1977) which emphasizes the use of multiple perspectives on data to help formulate hypotheses before proceeding to hypothesis testing. Visualizing probability distributions conditional on one or more granularities is a potentially useful approach for exploration. Analysts are expected to iteratively explore all possible choices of time granularities for comprehending possible periodicities in the data. But too many choices and a lack of a systematic approach to do so might become overwhelming.

Calendar-based graphics (Wang, Cook, and Hyndman 2018) are useful in visualizing patterns in the weekly and monthly structure well and are capable of checking the weekends or special days. Any sub-daily resolution temporal data can also be displayed using this type of faceting (Wickham 2016) with days of the week, month of the year and another sub-daily deconstruction of time. But calendar effects are not restricted to conventional day-of-week, month-of-year ways of deconstructing time. There can be several classes of time deconstructions, viz. based on the arrangement (linear vs. cyclic) or hierarchical order of the calendar. Linear time granularities respect the linear progression of time such as hours, days, weeks and months. One of the first attempts of characterizing these granularities occur in (Bettini et al. 1998). The definitions and rules defined are inadequate to reflect periodicities in time. Hence, there is a need to define cyclic time granularities in a different approach, which can be useful in visualizing periodic behavior. Cyclic time granularities can be circular or aperiodic depending on if mappings between granularities are regular or irregular. Examples of circular can be hour of the day, day of the week and that of aperiodic granularities can be day of the month or public holidays. Time deconstructions can also be based on the hierarchical structure of time. For example, hours are nested within days, days within weeks, weeks within months, and so on. Hence, it is possible to construct single-order-up granularities like second of the minute or multiple-order-up granularities like second of the hour. lubridate (G Grolemund 2011) creates easy access and manipulation of common date-time objects. But most accessor functions are limited to single-order-up granularities.

The motivation for this work comes from the desire to provide methods to better understand large quantities of measurements on energy usage reported by smart meters in households across Australia, and indeed many parts of the world. Smart meters currently provide half-hourly use in kWh for each household, from the time that they were installed, some as early as 2012. Households are distributed geographically and have different demographic properties such as the existence of solar panels, central heating or air conditioning. The behavioral patterns in households vary substantially, for example, some families use a dryer for their clothes while others hang them on a line, and some households might consist of night owls, while others are morning larks. It is common to see aggregates (Goodwin, S And Dykes, 2012), of usage across households, total kWh used each half hour by state, for example, because energy companies need to understand maximum loads that they will have to plan ahead to accommodate. But studying overall energy use hides the distributions of usage at finer scales, and making it more difficult to find solutions to improve energy efficiency. We propose that the analysis of smart meter data can be benefited from systematically exploring energy consumption by visualizing the probability distributions across different deconstructions of time to find regular patterns/anomalies. However, the motivation came through the smart meter example, this is a problem which relates to any data that needs to be analyzed for different periodicities.

This work provides tools for systematically exploring bivariate granularities within the tidy workflow through the following:

- Formal characterization of cyclic granularities
- Facilitate manipulation of single and multiple order-up time granularities
- Checking feasibility of creating plots or drawing inferences from any two cyclic granularities
- Recommend prospective probability distributions for exploring distributions of univariate dependent variable across pair of granularities

The remainder of the paper is organized as follows. Section ?? details the background of linear granularities in depth and introduces the characterization of circular and aperiodic time granularities. Section 5.1 discusses the effect in data structure due to how pairs of cyclic time granularities are related. Section 6 discusses the role of plot choices, synergy of time granularities and number of observations to construct an informative and trustworthy visualization. Section 7 discusses how systematic exploration can be carried out for a temporal and non-temporal case. Section 8 summarizes this paper and discusses possible future direction.

2 Linear Time granularities

Often we partition time into months, weeks or days to relate it to data. Such discrete abstractions of time can be thought of as time granularities (Aigner et al. 2011). Time granularities are **linear** if they respect the linear progression of time. Examples include hours, days, weeks and months.

2.1 Definitions and Relationships

There has been several attempts to provide the framework for formally characterizing time-granularities. One of the first attempts occur in (Bettini et al. 1998) with the help of the following definitions:

[section]

Definition 1 A time domain is a pair $(T; \leq)$ where T is a non-empty set of time instants and \leq is a total order on T .

A time domain can be **discrete** (if there is unique predecessor and successor for every element except for the first and last one in the time domain), or it can be **dense** (if it is an infinite set). A time domain is assumed to be discrete for the purpose of our discussion.

Definition 2 A linear granularity is a mapping G from the integers (the index set) to subsets of the time domain such that:

(1) if $i < j$ and $G(i)$ and $G(j)$ are non-empty, then each element of $G(i)$ is less than all elements of $G(j)$, and (2) if $i < k < j$ and $G(i)$ and $G(j)$ are non-empty, then $G(k)$ is non-empty.

Definition 3 Each non-empty subset $G(i)$ is called a granule, where i is one of the indexes and G is a linear granularity.

Dicussion: The first condition in 2 implies that the granules in a linear granularity are non-overlapping and their index order is same as time order. Figure 1 shows the implication of this condition. It shows the linear granularities hours, days, weeks, months and years, each of which are unidirectional in nature and arranged from past to future. If we consider the chronon (Aigner et al. 2011) as hourly, the time domain with T hours will have $\lfloor T/24 \rfloor$ days, $\lfloor T/(24 * 7) \rfloor$ weeks and so on. Each granule of the linear granularities shown are represented through a box.

(Bettini et al. 1998) talks about the relationships of linear time granularities and structure of a calendar and also relates them to the notion of periodicity in time.

Definition 4 A linear granularity G is finer than a linear granularity H , denoted $G \preceq H$, if for each index i , there exists an index j such that $G(i) \subset H(j)$.

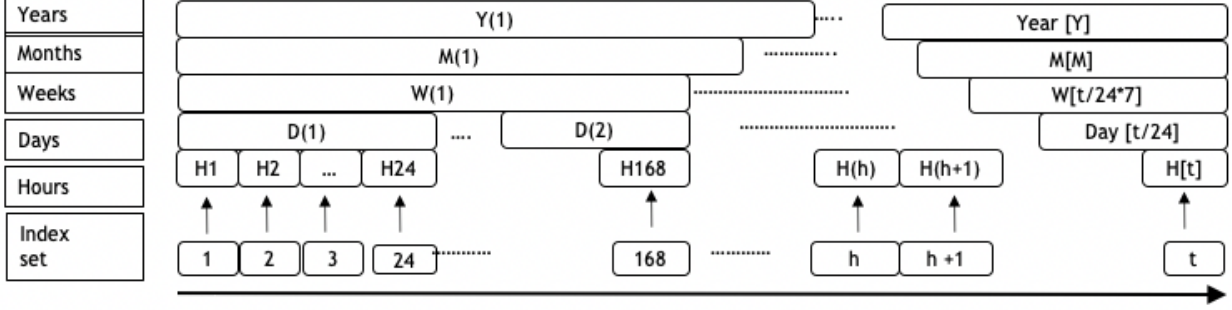


Figure 1: The time domain distributed as linear granularities

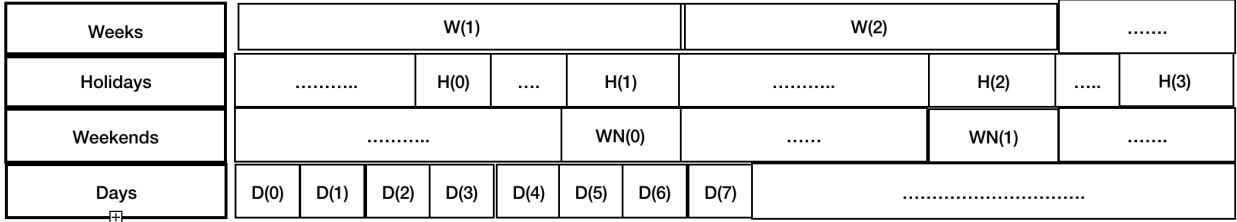


Figure 2: Illustrations of groups into and finer than relationships. Weekends groups into Holidays but Weekends are not finer than Holidays. On the other hand, Weekends are finer than weeks but do not group into weeks. Day groups into and are finer than weeks

Definition 5 A linear granularity G groups into a linear granularity H , denoted $G \leq H$, if for each index j there exists a (possibly infinite) subset S of the integers such that

$$H(j) = \bigcup_{i \in S} G(i) \quad (1)$$

Dicussion: $G \leq H$ if each granule $H(j)$ is the union of some granules of G . $G \preceq H$ if every granule in G is a subset of some granule in H . In Figure 2, both $Days \leq Weeks$ and $Days \preceq Weeks$ hold true. However, Weekends groups into Holidays but Weekends are not finer than Holidays. On the other hand, Weekends are finer than weeks but do not group into weeks. Consider another example where $Days \leq Months$. This relationship is not fully described until we associate it with periodicity. Each month is a grouping of the same number of days over years, hence the period of the grouping (day, month) is one year, if leap years are ignored. The period becomes 400 years with the inclusion of leap years and all their exceptions, .

Definition 6 A granularity H is periodical with respect to a granularity G if (1) $G \leq H$, and (2) there exist $R, P \in \mathbb{Z}^+$, where R is less than the number of granules of H , such that for all $i \in \mathbb{Z}$, if $H(i) = \bigcup_{j \in S} G(j)$ and $H(i + R) \neq \emptyset$ then $H(i + R) = \bigcup_{j \in S} G(j + P)$.

A granularity H which is periodical with respect to G is specified by: (i) the R sets of indexes of G , S_0, \dots, S_{R-1} describing the granules of H within one period; (ii) the value of P ; (iii) the indexes of first and last granules in H , if their value is not infinite. Then, if S_0, \dots, S_{R-1} are the sets of indexes of G describing $H(0), \dots, H(R-1)$, respectively, then the description of an arbitrary granule $H(j)$ is given by: $\bigcup_{i \in S_j \bmod R} G(P * \lfloor j/R \rfloor + i)$.

Dicussion:

Granularities can be periodical with respect to other granularities, except for a finite number of spans of time where they behave in an anomalous way (Bettini and De Sibi 2000).

Definition 7 A granularity H is quasi-periodical with respect to a granularity G if (1)

$$G \leq H,$$

, and (2) there exist a set of intervals E_1, \dots, E_z (the granularity exceptions) and positive integers R, P , where R is less than the minimum of the number of granules of H between any 2 exceptions, such that for all $i \in \mathbb{Z}$, if $H(i) = \bigcup_{k \in [0, k]} G(j_r)$ and $H(i + R) \neq \phi$ and $i + R < \min(E)$, where E is the closest existing exception after $H(i)^2$, then $H(i + R) = \bigcup_{k \in [0, k]} G(j_r + P)$.

Dicussion:

Intuitively, the definition requires that all granules of H within the span of time between two exceptions have the same periodical behavior, characterized by R and P .

Definition 8 Bottom granularity - Given a granularity order relationship $g\text{-rel}$ and a set of granularities having the same time domain, a granularity G in the set is a bottom granularity with respect to $g\text{-rel}$, if G $g\text{-rel}$ H for each granularity H in the set.

Dicussion: Given the set of all granularities defined over the time domain $(\mathbb{Z}; <)$, and the granularity relationship \leq (groups into), the granularity mapping each index into the corresponding instant (same integer number as the index) is a bottom granularity with respect to \leq .

2.2 Computation through Calendar Algebra

Linear time granularities are computed through an algebraic representation for time granularities, which is referred to as calendar algebra (Ning, Wang, and Jajodia 2002). It is assumed that there exists a “bottom” granularity and Calendar algebra operations are designed to generate new granularities from the bottom one or recursively, from those already generated. Thus, the relationship between the operand(s) and the resulting granularities are encoded in the operations.

The calendar algebra consists of two kinds of operations: grouping-oriented and granule-oriented operations. The grouping-oriented operations combine certain granules of a granularity together to form the granules of the new granularity. Example can be to consider a calendar with only two linear granularities minute and hour and hour is generated by grouping every 60 minutes. The granule-oriented operations do not change the granules of a granularity, but rather make choices of which granules should remain in the new granularity. For example, one can choose to look at the granularity “Monday” and hence select only Mondays while looking at the linear granularity “day”.

Some relevant grouping oriented operations are discussed, which will be used in Section 3 to define circular and aperiodic granularities.

- **The grouping operation** : Let G be a full-integer labeled granularity, and m a positive integer. The grouping operation $Group_m(G)$ generates a new granularity G , by partitioning the granules of G into m -granule groups and making each group a granule of the resulting granularity. More precisely, $G = Group_m(G)$ is the full-integer labeled granularity such that for each integer i , $G(i) = \bigcup_{j=(i-1)m+1}^{im} G(j)$.

Examples :

- $minute = Group_{60}(second)$
- $hour = Group_{60}(minute)$,
- $day = Group_{24}(hour)$,
- $week = Group_7(day)$,

where, second(1) would start a minute and likewise.

- **The altering-tick operation** : Let G_1, G_2 be full-integer labeled granularities, and l, k, m integers, where G_2 partitions G_1 , and $1 \leq l \leq m$. The altering-tick operation $Alter_{l,k}^m(G_2, G_1)$ generates a new full-integer labeled granularity by periodically expanding or shrinking granules of G_1 in terms of

granules of G2. The altering-tick operation modifies the granules of G1 so that the l th granule of each group has $|k|$ additional (or fewer when $k < 0$) granules of G2.

Example :

- pseudomonth = $Alter_{11,-1}^{12}(day, Alter_{9,-1}^{12}(day, Alter_{6,-1}^{12}(day, Alter_{4,-1}^{12}(day, Alter_{(2,-3)}^{12}(day, Group_{31}(day))))))$, where the granularity pseudomonth is generated by grouping 31 days, and then shrink April (4), June (6), September (9) and November (11) by 1 day, and shrink February (2) by 3 days. (Ning, Wang, and Jajodia 2002)

For more variations of grouping operations and granule oriented operations, the readers are recommended to see (Ning, Wang, and Jajodia 2002).

3 Cyclic Time granularities

We propose a formalism of cyclic time granularities through the tsibble (Wang, Cook, and Hyndman 2019) framework of organizing temporal data. A time domain, as defined by (Bettini et al. 1998), is essentially a mapping of the index set to the time index of a tsibble. A linear granularity is a mapping of the index set to subsets of the time domain. For example, if the time index is days, then a linear granularity might be weeks, months or years. Lining up with the assumption in (Bettini and De Sibi 2000) that all linear granularities can be generated from the bottom granularity by calendar algebraic operations, we assume that a bottom granularity exists and is represented by the index of the tsibble. In a cyclic organization of time, the domain is composed of a set of recurring time values, where any time value can be preceded and succeeded by another time value (for e.g Monday comes before Wednesday but Monday also succeeds Wednesday). Hence intuitively, cyclic granularities are additional abstractions of time which are not linear and hence the index order of linear granularities needs to be manipulated so that it leads to repetitive categorization of time.

Cyclic time granularities which accommodate periodicities can be constructed by relating two linear granularities. The mappings between linear granularities can be regular or irregular. For example, a regular mapping exists between minutes and hours, where 60 minutes always add up to 1 hour. On contrary, an irregular mapping exists between days and months, since one month can have days ranging from 28 to 31. To elaborate more, mappings will be regular if, for example, linear granularities are formed by grouping operation. Grouping operations combine fixed granules of a linear granularity to form a new granule of the resulting linear granularity. However, if granularities are formed by the altering-tick operation, for example, granules of the resulting granularity is composed of different number of granules of the root granularity. Cyclic time granularities are referred to as **circular** if mappings between linear time granularities are regular and **quasi-circular** if the same is irregular. Examples of circular granularities include hour of the day, and day of the week, whereas examples for quasi-circular granularities can be day of the month or week of the month. The formalisms would differ for circular and quasi-circular granularities although both accommodate periodicities in data.

3.1 Circular

Definition 9 A circular granularity $C(B, G)$ relates a linear granularity G to the bottom granularity B , if

$$C_{B,G}(z) = L(z \bmod k(B, G)) \quad \forall z \in \mathbb{Z}^+ \quad (2)$$

where,

z denotes the index set,

B denotes a full-integer labelled bottom granularity which groups periodically into linear granularity G with regular mapping,

L is a label mapping that defines a unique label for each index $l \in 0, 1, \dots, (k-1)$,

and $k(B, G)$ is the number of granules of B in each granule of G .

Discussion: In general, the set of labels will be a set of strings that is more descriptive than the index and used to identify a categorisation of the circular granularity. However, the labels can coincide with indexes in

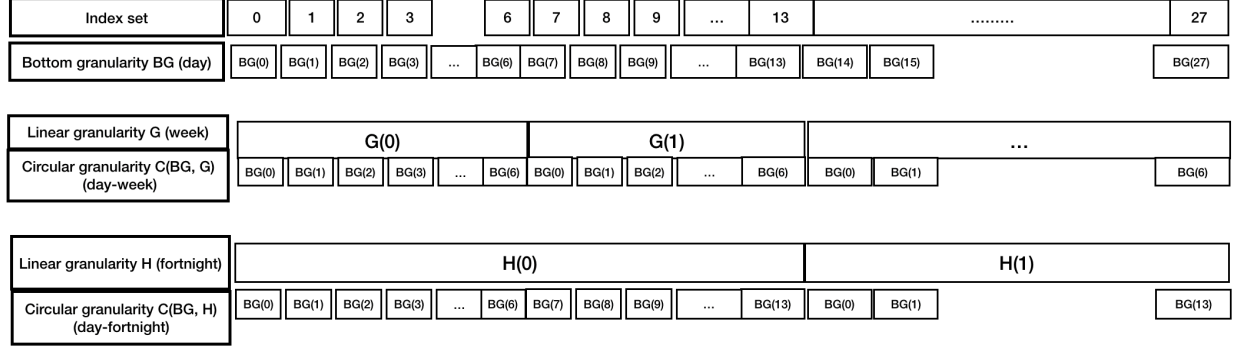


Figure 3: Relating circular granularities and bottom linear granularity

which case integers are directly used to refer to categorisations of the circular granularity. Note that each circular granularity can use a different set of labels. Example showing circular granularities relating two linear granularities each with bottom granularities are visually depicted in a series of slots in the Figure 3. Each granule is represented by a box. The diagram also illustrates that the granules that overlap share elements from the underlying time domain. The first slot in the diagram shows the index set and the bottom granularity. The index of the tsibble considered is days. G and H are two linear granularities denoting days and weeks respectively. $k(\text{day}, \text{week}) = 7$ and hence, $C_{G,B}(z)$ represented by $C(BG, G)$ is given by $B(z \bmod 7)$. The circular granularity $C(B, G)$ consists of repetitive pattern $\{L(0), L(1), L(2), L(3), L(4), L(5), L(6)\}$ which repeats itself after each period length. L can be defined such that the labels corresponding to $0, 1, \dots, 6$ correspond to different days of the week *Sun, Mon, \dots, Sat*. Similarly, $C(B, H)$ is given by $BG(z \bmod 14)$ since the period length of days with respect to fortnight is 14. $C(B, H)$ also repeats the pattern $L'(0), \dots, L'(13)$ in every period. Hence, circular granularities are represented as repetitive categorization of time in the diagram.

All circular granularities can be expressed in terms of the bottom linear granularity with equation Equation 2.

In general, any circular granularity relating two linear granularity, none of which are bottom granularity can be expressed as $C_{(G,H)}(z) = L(\lfloor z/k(B, G) \rfloor \bmod k(G, H))$, where linear granularity H is periodic with respect to linear granularity G and $k(G, H)$ represents the number of granules of G in one granule of H .

Table 1 shows representation of circular granularities relating two linear granularities. It is possible that none of these two linear granularities are bottom granularities. But the representation of the resultant circular granularity will be a function of the index set. Suppose the bottom granularity is minutes, k_i is the number of granules of the finer granularity in each granule of the coarser granularity in the circular granularity C_i and L_i is the associated label mapping.

Minute-of-Hour:	$C_1(z) = L_1(z \bmod 60)$	$k_1 = 60$
Minute-of-Day:	$C_2(z) = L_2(z \bmod 60 * 24)$	$k_2 = 1440$
Hour-of-Day:	$C_4(z) = L_3(\lfloor z/60 \rfloor \bmod 24)$	$k_3 = 24$
Hour-of-Week:	$C_6(z) = L_4(\lfloor z/60 \rfloor \bmod 24 * 7)$	$k_4 = 168$
Day-of-Week:	$C_7(z) = L_5(\lfloor z/24 * 60 \rfloor \bmod 7)$	$k_5 = 7$

Table 1: Illustrative circular granularities with time index in minutes

3.2 Quasi-circular

A **quasi-circular** granularity can not be defined using modular arithmetic due to its irregular mapping with the bottom granularity. For example, Table 2 shows some example of quasi-circular granularities (Q_i) and plausible choices of number of granules (k_i) of the finer granularity inside each granule of the coarser one in the cyclic granularity (Q_i).

Day-of-Month:	$Q_1(z)$	$k_1 = 31, 30, 29, 28$
Hour-of-Month:	$Q_2(z)$	$k_2 = 24 * 31, 24 * 30, 24 * 29, 24 * 28$
Day-of-Year:	$Q_3(z)$	$k_3 = 366, 365$
Week-of-Month:	$Q_4(z)$	$k_4 = 5, 4$

Table 2: Illustrative quasi-circular granularities with potential period lengths

Definition 10 A quasi-circular granularity $Q(B, G')$ that relates linear granularities G' and bottom granularity B , if

$$Q_{B,G'}(z) = L(z - \sum_{w=0}^{k-1} |T_w \bmod R'|), \quad z \in T_k \quad (3)$$

where, z denotes the index set,

B denotes a full-integer labelled bottom granularity which groups periodically into linear granularity G' with irregular mapping,

L is a label mapping that defines an unique label for each index $l \in 0, 1, \dots, (k-1)$,

T_w are the sets of indices of B describing $G'(w)$ such that

$$G'(w) = \bigcup_{z \in T_w} B(z), \quad (4)$$

$T_w = 0$ for $w \in Z_{<0}$,

$|T_w|$ is the cardinality of set T_w .

Since G' is periodical with respect to BG , from definition 6 the following holds true:

- $BG \trianglelefteq G'$
- $G'(w) = \bigcup_{z \in T_w \bmod R'} BG(P' * \lfloor w/R' \rfloor + z)$, where P' denotes the period of the grouping (BG, G') .

Discussion: Example showing quasi-circular granularities relating two linear granularities each with bottom granularities are visually depicted in a series of slots in Figure 4. Each granule is represented by a box. Similar to Figure 3, the granules that overlap share elements from the underlying time domain and the first slot shows the index set and the bottom granularity. Two linear granularities AG and AH are considered, where $G' = Alter_{(1,-1)}^2(BG, Group_3(BG))$ and $H' = Alter_{(1,-2)}^2(BG, Group_7(BG))$. This implies that G' is made up by shrinking every 1st granule of $Group_3(BG)$ by 1 granule and H' is made up of shrinking every 1st granule of $Group_3(BG)$ by 2 granules. Number of granules of G' and H' in each period of BG is 2, but the number of granules of BG in each of those granules are different. $QC(BG, G')$ and $QC(BG, H')$ are repetitive categorization of time, similar to circular granularities, except that the number of granules of BG is not necessarily the same across different granules of G' or H' . For G' , $R' = 2$, $P' = 5$, $T_0 = \{0, 1\}$ and $T_1 = \{2, 3, 4\}$. For H' , $R' = 2$, $P' = 12$, $T_0 = \{0, 1, 2, 3, 4, 5, 6\}$ and $T_1 = \{7, 8, 9, 10, 11\}$, then we will have Equation 5 and Equation 6.

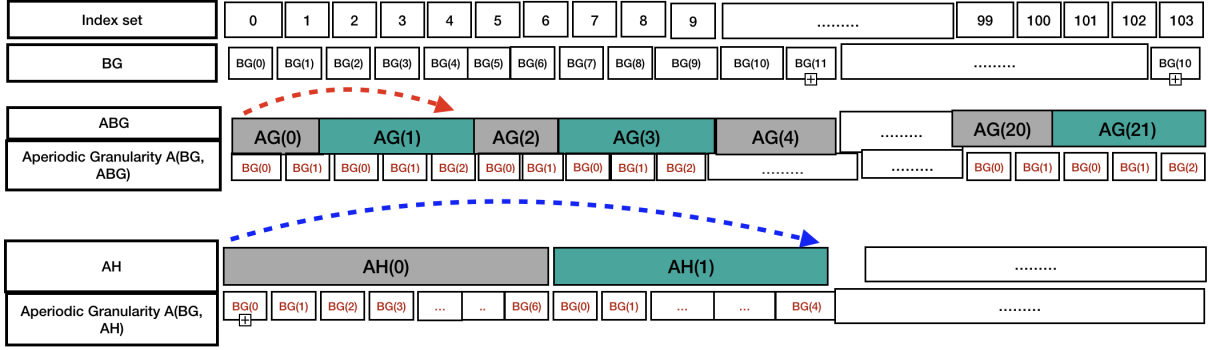


Figure 4: Relating quasi-circular granularities and bottom linear granularity

$$\begin{aligned}
 QC(BG, G')(8) &= BG(8 - \sum_{w=0}^{3-1} |T_w \bmod 2|), 8 \in T_3 \\
 &= BG(8 - \sum_{w=0}^2 |T_w \bmod 2|) \\
 &= BG(8 - \sum_{w=0}^2 |T_w \bmod 2|) \\
 &= BG(8 - |T_0 \bmod 2| - |T_1 \bmod 2| - |T_2 \bmod 2|) \\
 &= BG(8 - 2 * |T_0 \bmod 2| - |T_1 \bmod 2|) \\
 &= BG(8 - 2 * 2 - 3) \\
 &= BG(1)
 \end{aligned} \tag{5}$$

$$\begin{aligned}
 QC(BG, H')(10) &= BG(10 - \sum_{w=0}^{1-1} |T_w \bmod 2|), 10 \in T_1 \\
 &= BG(10 - \sum_{w=0}^0 |T_w \bmod 2|) \\
 &= BG(10 - |T_0 \bmod 2|) \\
 &= BG(10 - |T_0|) \\
 &= BG(10 - 7) \\
 &= BG(3)
 \end{aligned} \tag{6}$$

If we ignore leap years and all its exception, the periodicity of the grouping (days, months), $P' = 365$, $R' = 12$, since each month would be defined as the grouping of the same number of days (31, 28, or 30, depending on the month) every year. Considering leap years and all their exceptions, period is 400 years and hence $P' = (3 * 365 + 366)$, $R' = 12 * 400$. Equation 3 can be useful to find the aperiodic granularity day-of-month in both of these cases, since the grouping is periodic in both cases.

The linear granularities G , H , AG and AH considered in the definitions of circular and aperiodic granularities are all periodic with respect to the bottom granularity. The only difference is G , H have regular mapping, whereas, $G1$ and $G2$ have irregular mapping with respect to BG . It can be noted here that if a linear

Index set	0	1	2	3	4	5	6	7	8	9					99	100	101	102	103
BG	BG(0)	BG(1)	BG(2)	BG(3)	BG(4)	BG(5)	BG(6)	BG(7)	BG(8)	BG(9)	BG(10)	BG(11)					BG(103)		
G''																				
Aperiodic Granularity A(BG, G'')																				
	G''(0)		G''(1)				G''(2)			
	1	1	0	0	0	0	0	1	1	1	1	1	1	0	0	0	0	0	

Figure 5: Relating aperiodic granularity and bottom linear granularity

granularity AG is quasi-periodic with respect to BG, then Equation 3 can be modified as follows to account for exceptions $E = [e_{begin}, e_{end}]$ (by Definition 7).

$$A_{BG,AG}(z) = BG(z - \sum_{w=0}^{k-1} |T_w \bmod R'| - \sum_{u=0}^{e_k} |E_u|) \quad (7)$$

for $z \in T_k$ and e_k is the number of exceptions in $\bigcup_{w=0}^k T_w$ and $E_u = [e_{begin}(u), e_{end}(u)]$.

3.3 Aperiodic

Periodic and Quasi-periodic behavior can be defined by a repeating pattern, except for a finite number of granules that can be seen as discontinuity points in the granularity in case of quasi-periodic behavior. Aperiodic time granularities are the ones which can not be specified as a periodic repetition of a pattern of granules. Most public holidays repeat every year, but there is no period within which their behavior remains constant. A classic example can be that of Easter, whose dates repeat only after 5,700,000 years. U.S labour day is the first Monday in September and U.S. Memorial Day is the last day in May. In Australia, if a standard public holiday falls on a weekend, a substitute public holiday will sometimes be observed on the first non-weekend day (usually Monday) after the weekend. Examples of aperiodic granularity may also include school holidays or a scheduling event that might cover the first and third Monday of the month between June and October, except for state holidays. All of these are recurring events, but with non-periodic patterns. As such, plausible k_i from Table 2 can be infinite for aperiodic granularities.

\begin{timedom} An aperiodic granularity $A_{BG, G''}$ that relates linear granularities G and bottom granularity BG , with G'' being aperiodical with respect to BG , is given by

$$A_{BG, G''}(z) = 1, z \in T_q \\ = 0, z \notin T_q \quad (8)$$

where,

z denotes the index set (index of BG), T_q are the sets of indices of BG describing $G''(q)$ such that $G''(q) = \bigcup_{z \in T_q} BG(z), T_q = 0$ for $q \in Z_{<0}$. \end{timedom}

Discussion: Aperiodic time granularities map a time index to a categorical variable containing binary values. It takes the value 1 whenever the time index coincides with the events in context (e.g. public or school holiday) and 0 when it does not. Here, 1 and 0 are proxies to denote the binary categorization and can be replaced with a logical vector. An example of aperiodic granularity can be one that relates a bottom granularity (BG) and linear granularity (G'') such that $BG \trianglelefteq G''$, $BG \not\trianglelefteq G$ and BG is not periodic or quasi-periodic with respect to G'' , as shown in Figure 5.

4 Computing cyclic time granularities

The hierarchical structure of time creates a natural nested ordering which can produce **single-order-up** or **multiple-order-up** granularities. We shall use the notion of a hierarchy table and order to define them.

Definition: Order of a linear granularity can be comprehended as the level of graininess associated with a linear granularity. If we consider two linear granularities G and H , such that G is finer than or groups into H (by Definitions 4, 5), then H is of higher order than G .

Notation: Hierarchy table Let $H_n : (G, C, k)$ be a hierarchy model containing n linear granularities. G_l represents the linear granularity of order l and $k(l, m)$ represents the period length of G_l with respect to G_m and $C_{G(l), G(m)}$ represents the circular granularity that relates linear granularity of order l and m , $\forall l, m \in n, l < m$.

In a hierarchy table, linear granularities are arranged from lowest to highest order of linear granularities.

We refer to granularities which are nested within multiple levels as **multiple-order-up** granularities and those concerning a single level as **single-order-up** granularities. Let us look at few calendars to see examples of single and multiple order-up granularities.

4.1 Multiple-order from single-order

$$\begin{aligned}
C_{(G_l, G_m)}(z) &= C_{G_l, G_{l+1}}(z) + k(l, l+1)(C_{(G_{l+1}), G_m}(z) - 1) \\
&= C_{(G_l, G_{l+1})}(z) + k(l, l+1)[C_{G_{l+1}, G_{l+2}}(z) + k(l+1, l+2)(C_{G_{l+2}, G_m}(z) - 1) - 1] \\
&= C_{(G_l, G_{l+1})}(z) + k(l, l+1)(C_{G_{l+1}, G_{l+2}}(z) - 1) + k(l, l+1)k(l+1, l+2)(C_{G_{l+2}, G_m} - 1) \\
&= C_{(G_l, G_{l+1})}(z) + k(l, l+1)(C_{G_{l+1}, G_{l+2}}(z) - 1) + k(l, l+2)(C_{G_{l+2}, G_{l+m}}(z) - 1) \\
&\vdots \\
&= \sum_{i=0}^{m-l-1} k(l, l+i)(C_{G_{l+i}, G_{l+i+1}}(z) - 1)
\end{aligned} \tag{9}$$

Example: So far we have used the Gregorian calendar as it is the most widely used calendar. But it is far from being the only one. All calendars fall under three types - solar, lunar or lunisolar/solilunar but the day is the basic unit of time underlying all calendars. Various calendars, however, use different conventions to structure days into larger units: weeks, months, years and cycle of years. The French revolutionary calendar divided each day into 10 “hours”, each “hour” into 100 “minutes” and each “minute” into 100 “seconds”. Nevertheless, for any calendar a hierarchy can be defined. For example, in Mayan calendar, one day was referred to as 1 kin and the calendar was structured as follows (Reingold and Dershowitz 2001):

- 1 kin = 1 day
- 1 uinal = 20 kin
- 1 tun = 18 uinal
- 1 katun = 20 tun
- 1 baktun = 20 katun

Thus, the hierarchy table for the Mayan calendar would look like the following:

G	C	k
kin	kin-of-uinal	20
uinal	uinal-of-tun	18
tun	tun-of-katun	20
katun	katun-of-baktun	20
baktun	1	1

Examples of multiple-order-up granularities can be kin-of-tun or kin-of-baktun whereas examples of single-order-up granularities may include kin-of-uinal, uinal-of-tun etc.

Let us use the equation 3 to compute the multiple-order-up granularity uinal_katun for Mayan calendar, which is periodic and regular.

$$\begin{aligned} C(uinal, baktun) &= C(uinal, tun) + kuinal, tun C(tun, katun) + C(uinal, katun) C(katun, baktun) \\ &= \lfloor z/20 \rfloor \mod 18 + 20 * \lfloor z/20 * 18 \rfloor \mod 20 + 20 * 18 * 20 \lfloor z/20 * 18 * 20 \rfloor \mod 20 \end{aligned} \quad (10)$$

4.2 Single-order from multiple-order

For a hierarchy table $H_n : (G, C, k)$ with $l_1, l_2, m_1, m_2 \in 1, 2, \dots, n$ and $l_2 < l_1$ and $m_2 > m_1$, we have

$$C_{G_{l_1}, G_{m_1}}(z) = C_{G_{l_2}, G_{m_2}}(\lfloor z/k(l_2, l_1) \rfloor \mod k(m_1, m_2)) \quad (11)$$

Example: Considering the same example of Mayan Calendar, it is possible to compute the single-order-up granularity tun-of-katun given the multiple-order-up granularity uinal-baktun using equation 6

$$C(tun, katun) = \lfloor C(uinal, baktun)(z)/18 \rfloor \mod 20 \quad (12)$$

In subsection 4.2 and subsection 4.1, we assume that all single order granularities are circular. What happens when we have a mix of circular and aperiodic granularities.

Let us turn to Gregorian calendar for addressing this case. Suppose we have a hierarchy table using some linear granularities from Gregorian calendar. Since months consists of unequal number of days, any temporal unit which is higher in order than months will also have unequal number of days. This is an example of a hierarchy structure which has both circular and aperiodic single-order-up granularities. The single-order-up granularity day_month is aperiodic. Any single-order-up granularities which are formed by units below days are periodic. Similarly, all single-order-up granularities which are formed using units whose orders are higher than months are also periodic.

G	C/A	k
minute	minute-of-hour	60
hour	hour-of-day	24
day	day-of-month	“aperiodic”
month	month-of-year	12
year	1	1

There can be three scenarios for obtaining multiple-order-granularities here: - granularities relating two linear granularities whose orders are less than day - granularities relating two linear granularities whose orders are more than month - granularities relating two linear granularities with order at most day and another with order at least month

The single order-up granularities resulting from the first two cases are periodic and has been handled in subsection 4.2 and subsection 4.1. The calendar categorization resulting from the last case are aperiodic. Examples might include day of the quarter or hour of the month. Let us consider the computation of $A_{hour, month}$ given single order-up granularities $A_{hour, day} = 12$, $A_{day, month} = 20$ and $C_{month, year} = 9$.

$$\begin{aligned}
A_{(hour, month)} &= \left(\sum_{w=0}^{9-1} (|T(w)|) + 20 \right) / 24 + 12 \\
&= \left(\sum_{w=0}^{C_{month, year} - 1} (|T(w)|) + A_{day, month} \right) * k(hour_{day}) + A_{hour, day} \\
&= (A_{day, year} - 1) * k(hour_{day}) + A_{hour, day}
\end{aligned} \tag{13}$$

where, $month(w) = \bigcup_{z \in T_w} day(z)$

Clearly, the computation of multiple order-up granularities become more involved with aperiodic mappings of linear granularities in the calendar structure. With one aperiodic granularity, we can write the following:

$A_{\{P, Q\}} \& = (A_{\{AG_Q\}} - 1) * k(P_AG) + A_{\{P, AG\}}$ {TO REVISE: many aperiodic granularities not to be included}

5 Data structure

Effective exploration or good visualization require good data structures. Commonly, simple sequences of time value pairs $\langle t_0, v_0 \rangle, \dots, \langle t_n, v_n \rangle$ are the basis of analysis and visualization. It is recognized that the initial approaches of just considering time as an ordinal dimension in visualisation are inadequate to capture characteristics of time-dependent information. There is a crucial influence of linear vs cyclic time characteristics on the expressiveness of visualization and analysis. Moreover, one can use calendars based on application domain that define contextual system of granularities. Data can then be consolidated for different levels of granularity enabling statistical summaries of values along granularities. Since, we are interested in detection of previously unknown periodic behavior of data, it makes sense to support the detection of patterns by obtaining statistical summaries across cyclic time granularities. Any attempt to encode all or many cyclic granularities at the same time to develop insights on periodicity might fail or become clumsy. Instead, the big problem can be broken down into smaller pieces by focusing on two cyclic granularities at a time.

A recent tidy data structure to support exploration and modeling of temporal data is tsibble (Wang, Cook, and Hyndman 2019), where data is structured in a semantic manner with reference to observations and variables, with the time index stated explicitly. Since all cyclic granularities can be expressed in terms of the bottom granularity, which is the index of the tsibble, we consider the data structure in (Figure 6 for exploration of temporal data of this kind. This is extending the columns of tsibble by including the cyclic granularities. Now suppose we want to explore the measurement variable v across two cyclic granularities C_1 and C_2 , such that C_1 maps index set to a set $\{A_1, A_2, A_3, \dots, A_n\}$, and C_2 maps index set to a set $\{B_1, B_2, B_3, \dots, B_m\}$. Also, let S_{ij} be the set of index set such that for all $s \in S_{ij}$, $C_1(s) = A_i$ and $C_2(s) = B_j$. Data subsets like $\langle A_i, B_j, v(s) \rangle$ can be obtained for all $i \in 1, 2, \dots, n$ and $j \in 1, 2, \dots, m$ which will lead to nm such sets. These sets can form the basis for exploration and analysis of the measured variable across these bivariate cyclic granularities.

index	cyclic granularity 1	cyclic granularity 2	key	measurements

Figure 6: The data structure for exploring periodicities in data. Two cyclic granularities serve as fixed and conditioned variable and the measurement variable is the observation across combinations of these cyclic time granularities.

5.1 Synergy of the cyclic granularities

The way cyclic granularities relate become important when we consider the data structure $\langle A_i, B_j(s), v(s) \rangle$ for exploration. We will discuss few cases, where one or more of these nm sets will be empty, which will essentially mean that the measured variable can not be explored for all combinations of the levels of the cyclic granularities. To consider a general framework, we will define pairs of cyclic granularities as harmonies or clashes.

Firstly, empty combinations can arise due to the structure of the calendar or hierarchy. These are called “structurally” empty combinations. Let us take a specific example, where C_1 maps row numbers to Day-of-Month and C_2 maps row numbers to Week-of-Month. Here C_1 can take 31 values while C_2 can take 5 values. There will be $31 \times 5 = 155$ sets S_{ij} corresponding to the possible combinations of WOM and DOM. Many of these are empty. For example $S_{1,5}$, $S_{21,2}$, etc. This is also intuitive since the first day of the month can never correspond to fifth week of the month. These are structurally empty sets in that it is impossible for them to have any observations.

Secondly, empty combinations can turn up due to differences in event location or duration in a calendar. These are called “event-driven” empty combinations. Again, let us consider a specific example to illustrate this. Let C_1 be DOW and C_2 be WorkingDay/NonWorkingDay. Here C_1 can take 7 values while C_2 can take 2 values. So there are 14 sets S_{ij} corresponding to the possible combinations of DOW and WD/NWD. While potentially all of these can be non-empty (it is possible to have a public holiday on any DOW), in practice many of these combinations will probably have very few observations. For example, there are few if any public holidays on Wednesdays or Thursdays in any given year in Melbourne.

Thirdly, empty combinations can be a result of how granularities are constructed. Let C_1 maps row numbers to “Business days”, which are days from Monday to Friday except holidays and C_2 is Day-of-Month. Then the weekends in Days-of-Month would not correspond to any Business days and would have missing observations due to the way the granularities are constructed. This is different from the structurally empty combinations because structure of the calendar does not lead to these missing combinations, but the construction of the granularity does. Hence, they are referred to as “build-based” empty combinations.

An example when there will be no empty combinations could be where C_1 maps row numbers to Day-of-Week and C_2 maps row numbers to Month-of-Year. Here C_1 can take 7 values while C_2 can take 12 values. So there are $12 \times 7 = 84$ sets S_{ij} corresponding to the possible combinations of DOW and MOY. All of these are non-empty because every DOW can occur in every month.

Therefore, pair of cyclic granularities which lead to structurally, event-driven or build-based empty-combinations are referred to as to as **clashes**. And the ones that do not lead to any missing combinations are called **harmonies**.

5.2 Density estimation of measured variable

The measured variable can be discrete or continuous. The probability distribution of these univariate measured variable could be studied by estimating the probability density function (pdf for continuous) or probability mass function (pmf for discrete). Both pdf and pmf are concerned with point probabilities of the random variable. Suppose we have observations which are realizations of univariate random variables, $X_1, X_2, \dots, X_n \sim F$, where F denotes an unknown cumulative distribution function and X_1, X_2, \dots, X_n are i.i.d. The densities can either be estimated or summarized using quantiles. Instead of assuming a parametric model for the distribution (e.g. a Normal distribution with unknown expectation and variance), a non-parametric estimation assumes that the density exists and is suitably smooth (e.g. differentiable). It is then possible to estimate the unknown density function $f(\cdot)$.

The histogram is the oldest and most popular density estimator method. The form of the histogram depends very much on the tuning parameters class width and origin. The naive estimator was introduced by Fix and Hodges (1951) and first discussed by Rosenblatt (1956). Whittle (1958) formulated the general weight function class of estimators, while the orthogonal series estimator was introduced by Cencov (1962). The nearest neighbour estimate considered by Loftsgaarden and Quesenbury (1965), while the variable Kernel method is due to Brieman, Meisel and Purcell (1977). There are quite a few other approaches to density

estimation than the kernel estimators, but the fixed bandwidth kernel estimators are used predominantly because of their simplicity.

The quantile of a distribution is defined as $Q(p) = F^{-1}(p) = \inf x : F(x) > p$, $0 < p < 1$, where $F(x)$ is the distribution function. Let $X_{(1)}, \dots, X_{(n)}$ denote the order statistics of X_1, X_2, \dots, X_n , and let $Q_i(p)$ denote the i th sample quantile definition, then

$$Q_i(p) = (l - \gamma)X_{(j)} + \gamma X_{(j+1)} \quad (14)$$

where, $(j - m)/n \leq p < (j - m + 1)/n$

There have been several other nonparametric quantile estimators proposed e.g., Harrell and Davis 1982; Sheather and Marron 1990). Also sample quantiles can be of the form that are not defined for all p including hinges, letter values (Hoaglin 1983) and related methods (Freund and Perles 1987).

6 Visualization

Creating a visualisation requires a number of nuanced judgements. We exploit some features of layers and faceting (Wilkinson 1999) and (Wickham 2016) to come up with a recommendation system while visualizing the distribution of the “dependent” variable across bivariate temporal granularities. The general framework of visualizing the distribution involves a faceting approach with one temporal granularity plotted along the x-axis, the other one across facet and the dependent time series variable on the y-axis. Different distribution plots might be appropriate depending on which features of the distribution we are interested to look at, the levels of time granularities being plotted, how granularities interact and number of observations available. We will look at each of these aspects separately and analyze the effect of each on visualization.

While we accomplish that, we need to bear in mind that any customized species of visualization might be constructed by varying the set of mappings between data properties and visual attributes such as position, shape and color. We are trying to address problems where even with good aesthetic qualities and good data, the graph might be confusing or misleading because of how people process the information.

6.1 Choice of Plots

There are several ways to plot statistical distributions. The displayed probabilities in these plots are either computed using kernel density estimation methods or empirical statistical methods. The latter do not allow us to see the shape, skewness, nature of the tail or multi-modality with so much clarity as the former. However, they avoid much clutter, where some specific probabilities representing typical and extreme behavior are on focus. The probabilities displayed are based on actual data, which is aligned to principles that governed Tukey’s original boxplot. Density plots which uses a kernel density estimate to show the probability density function of the variable can show the entire distribution, unlike discretizing the distribution and showing only parts of it. They can be useful in spotting multimodality, however, they might become obscuring with too many categories and information on the entire distribution can add to cognitive load. Also, the probabilities in density plot are estimated through kernel density estimation and thus makes assumptions when selecting kernel or bandwidth. As a result, the plot shows smooth summaries based on the assumptions and not only on actual observations. The density based visualizations are subject to the same sample size restrictions and challenges that apply to any density estimation. In practice, the densities are estimated reasonably with at least 30 observations. Even with sample sizes of several hundred, however, choosing too large a value for bandwidth can cause the estimate to oversmooth the data.

We will discuss few conventional and recent ways to plot distributions using both of these methods.

6.1.1 Quantile based methods

Most commonly used techniques to display a distribution of data include the histogram (Karl Pearson), which shows the prevalence of values grouped into bins and the box-and-whisker plots (Tukey 1977) which convey

statistical features such as the median, quartile boundaries, hinges, whiskers and extreme outliers. The box plot is a compact distributional summary, displaying less detail than a histogram. Due to wide spread popularity and simplicity in implementation, a number of variations are proposed to the original one which provides alternate definitions of quantiles, whiskers, fences and outliers. Notched box plots (Mcgill, Tukey, and Larsen 1978) has box widths proportional to the number of points in the group and display confidence interval around medians aims to overcome some drawbacks of box plots. The standard box plot and all of these variations are helpful to get an idea of the distribution at a glance. Moreover, for data less than 1000 observations, detailed estimates of tail behavior beyond the quartiles are not trustworthy. Also, the number of outliers is large for larger data set since number of outliers is proportional to the number of observations.

The letter-value box plot (Hofmann, Wickham, and Kafadar 2017) was designed to adjust for number of outliers proportional to the data size and display more reliable estimates of tail. “outliers” in letter value plots are those observations beyond the most extreme letter value. The letter values are shown till the depths where the letter values are reliable estimates of their corresponding quantiles and hence might lead to a lot of letter values being shown and leading to overload of information in one plot.

Quantile plots visually portray the quantiles of the distribution of sample data. Much like the quartiles divide the data set equally into four equal parts, extensions include dividing the data set even further. These plots are referred to as “quantile” plots. For example, number of quantiles would be 9 for a decile plot and 99 for percentile plot. It avoids much clutter and just enable us to focus on specific probabilities, typically representing typical and extreme behaviors. A large data set is required for the extreme percentiles to be estimated with any accuracy. These plots can display any quantiles instead of quartiles in a traditional boxplot. When reviewing a boxplot, an outlier is defined as a data point that is located outside the fences (“whiskers”) of the boxplot (e.g: outside 1.5 times the interquartile range above the upper quartile and below the lower quartile). However, outliers are open to interpretation and not shown in an quantile plot.

6.1.2 Kernel density estimation methods

Traditional ways to visualize densities include violin plots (Hintze and Nelson 1998). The shape of the violin represents the density estimate of the variable. The more data points in a specific range, the larger the violin is for that range. Adding two density plots gives a symmetric plot which makes it easier to see the magnitude of the density and compare across categories, enabling easier detection of clusters or bumps within a distribution.

The summary plot (Potter et al. 2010, 2010) combines a minimal box plot with glyphs representing the first five moments (mean, standard deviation, skewness, kurtosis and tailings), and a sectioned density plot crossed with a violin plot (both color and width are mapped to estimated density), and an overlay of a reference distribution. This suffers from the same problem as boxplots or violin plot, as it is combination of those two.

A Ridge line plot (sometimes called Joy plot) shows the distribution of a numeric value for several groups. Distribution can be represented using histograms or density plots, all aligned to the same horizontal scale and presented with a slight overlap. A clear advantage over boxplots is that these plots allow us to see multimodality in the distribution. However, these plots can be obscuring when there is overlap of distribution for two or more categories of the y-axis. Also, if there are lot of categories, it is difficult to compare the height of the densities across categories.

The highest density region (HDR) box plot proposed by (Hyndman 1996) displays a probability density region that contains points of relatively highest density. The probabilities for which the summarization is required can be chosen based on the requirement. These regions do not need to be contiguous and help identify multi-modality.

Given a context, it is good to be conversant with the benefits and challenges while choosing a distribution plot. As a general rule, if we have too many categories, the quantile plots are useful for comparing patterns, whereas, other more involved methods of plotting are useful for studying anomalies, outlier or multimodal behavior.

6.1.3 Effect of levels of temporal granularities

The levels of the two granularities plotted have an impact on the choice of plots since space and resolution might become a problem if the number of levels are too high. The criteria for different levels could be based on usual cognitive power while comparing across facets and display size available to us. Plot choices will also vary depending on which granularity is placed on the x-axis and which one across facets.

Levels are categorized as very high/high/medium/low each for the facet variable and the x-axis variable. Default values for these levels are chosen based on levels of common temporal granularities like day of the month, day of a fortnight or day of a week. Any levels above 31 can be considered as very high, any levels between 14 to 31 can be taken as high and that between 7 to 14 can be taken as medium and below 7 as low. 31, 14 and 7 are the levels of days-of-month, days-of-fortnight and days-of week respectively.

The following principles are useful while choosing distribution plots given two temporal granularities.

- If levels of both granularity plotted are low/medium, then any distribution plots might be chosen depending on which feature of the distribution needs focus.
- If level of the granularity plotted across x-axis is more than medium, ridge plots should be avoided to escape overlap of categories.
- If level of the granularity plotted across x-axis is more than or equal to high, quantile plots are preferred.
- If levels of any granularity plotted are more than medium, empirical based methods of distribution visualizing are preferred as they use less space by design than most density based methods.

6.2 Effect of synergy of time granularities

In Section 5.1, we discussed how pairs of granularities can have empty combinations either due to structure of calendar, event location or duration or due to the way they are built. In this section, we will see how these empty combinations affect the visualization when a dependent variable is plotted against these granularities.

For illustration, distribution of half-hourly electricity consumption of Victoria is plotted across different time granularities in each of the panel in Figure 7. Figure 7 (a) shows the letter value plot across days of the month faceted by months like January, March and December. Figure 7 (c) shows box plot across days of the year by the 1st, 15th, 29th and 31st days of the month. Figure 7 (d) showing violin plot across days of the month faceted by week of the month. Figure 7 (e), variations across week of the year conditional on week of the month can be observed through a ridge plot and Figure 7 (f) shows decile plots across day of the year and month of the year.

Clearly, in Figure 7, we observe that some choices of time granularities work and others do not. In Figure 7 (c), there will be no observations for some combinations “Day-of-Month” and “Day-of-Year”. In particular, the 1st day of the month can never correspond to 2nd, 3rd or 4th day of the year. On the contrary, for Figure 7 (a), we will not have any combinations with zero combinations because every “Day-of-Week” can occur in any “Month-of-Year”. Thus the graphs that don’t work are those where many of the combination sets are empty. In other words, if there are levels of time granularities plotted across x-axis which are not spanned by levels of the time granularities plotted across facets or vice versa, we will have empty sets leading to potential ineffective graphs. We hypothesize that the synergy of these granularities are in play while deciding if the resulting plot would be a good candidate for exploratory analysis.

We redefine harmony and clashes as follows: harmonies are pairs of granularities that aid exploratory data analysis, and clashes are pairs that are incompatible with each other for exploratory analysis. As a result, we should avoid plotting clashes as they hinder the exploratory process by having missing combinations of time granularities in each panel.

6.3 Effect of number of observations

Even with harmonies, visualizing probability distributions can be misleading either due to rarely occurring categories or unevenly distributed events.

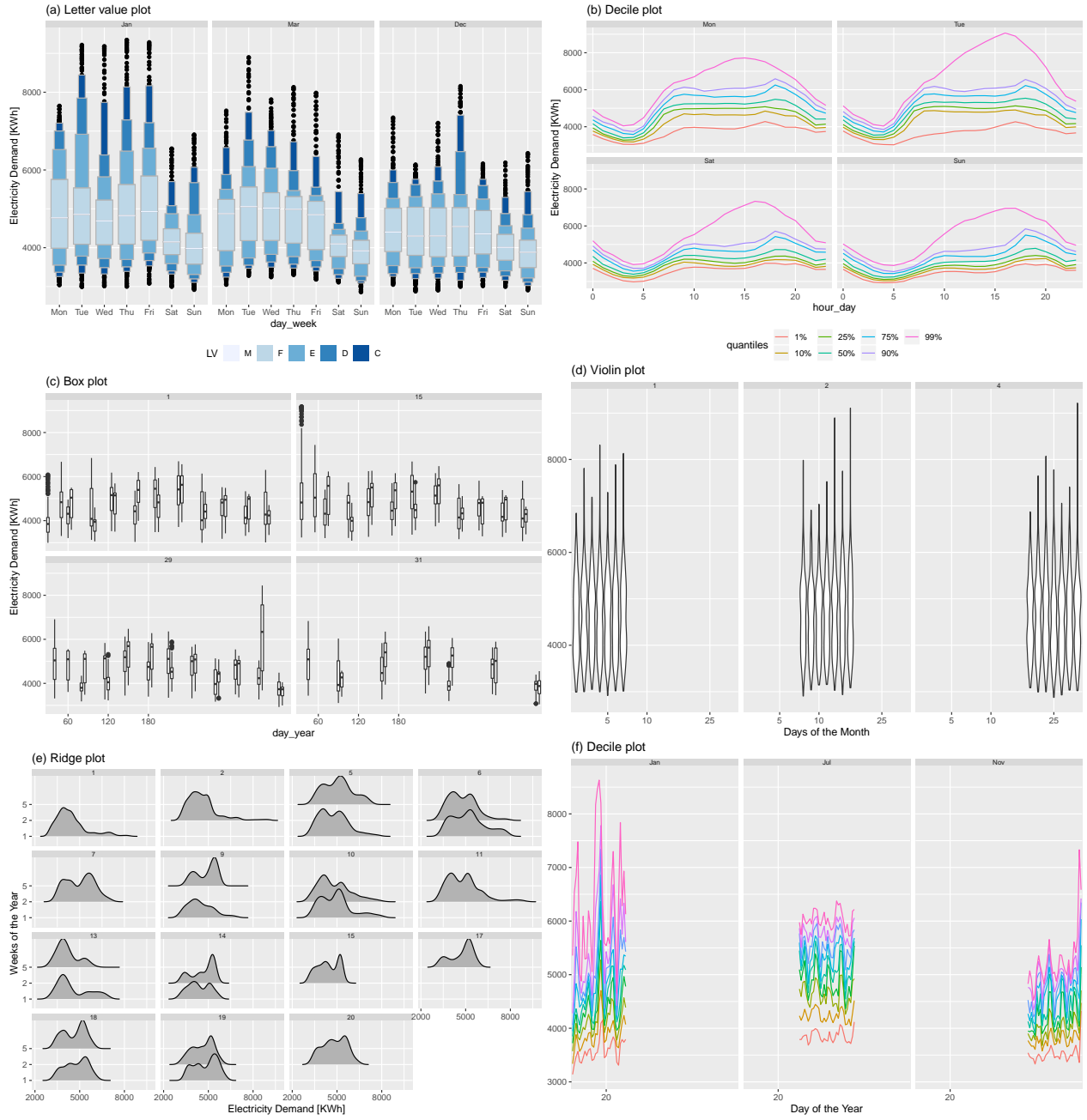


Figure 7: Various probability distribution plots of electricity consumption data of Victoria from 2012 to 2014. (a) Letter value plot by DoM and MoY, (b) Decile plot by HoD and DoW (c) Box plot by DoY and DoM, (d) Violin plot of DoM and WoM, (e) Ridge plot by WoM and WoY, (f) Decile plot by DoY and MoY. Only plots (a) and (b) show harmonised time variables.

6.3.1 Rarely occurring events

Suppose we have T observations, and two cyclic granularities - C_1 with n categories and C_2 with m categories. Each element of C_1 occurs approximately T/n times while each element of C_2 occurs approximately T/m times. There are no structurally empty combinations, and each combination will occur on average an equal number of times as $T \rightarrow \infty$, so the average number of observations per combination is $T/(mn)$. If we require at least k observations to create a meaningful panel, then provided $T \geq mnk$, the visualization will be acceptable. The value of k will depend on what type of visualization we are producing. For a decile plot, even $k = 10$ may be acceptable, but for density estimates, we would need $k \geq 30$. Rarely occurring categories such as the 366th day of the year, or the 31st day of the month can suffer from such problem.

6.3.2 Unevenly distributed events

Even when there are no rarely occurring events, number of observations might vary hugely within or across each panel. This might happen due to missing observations in the data or uneven locations of events in time domain. In such cases, the visualizations that use kernel density estimates should be used with caution as sample size would directly affect both the variance of the estimator and the confidence intervals. Measures such as Gini's coefficient may be used to see if sample sizes vary widely across panels.

7 Applications

7.1 Smart meter data of Australia

Smart meters provide large quantities of measurements on energy usage for households across Australia. One of the customer trial (Department of the Environment and Energy 2018) conducted as part of the Smart Grid Smart City (SGSC) project (2010-2014) in Newcastle, New South Wales and some parts of Sydney provides customer wise data on half-hourly energy usage and detailed information on appliance use, climate, retail and distributor product offers, and other related factors. It would be interesting to explore the energy consumption distribution for these customers and gain more insights on their energy behavior which are otherwise lost either due to aggregation or looking only at coarser temporal units. The idea here is to show how looking at the time across different granularities together can help identify different behavioral patterns and identify the extreme and regular households amongst these 50 households.

In Figure 8, the smart meter data is filtered for two customers to illustrate what kinds of insights can be drawn for the energy behavior of these two customers. it can be seen that for most days of the fortnight, the second household has much less consumption than the first one. However, there is additional information that we can derive looking at the distribution. If we consider letter value F as a regular behavior and letter values beyond F as not-so-regular behavior, we can conclude that the regular behavior of the first household is more stable than the second household. However, the distribution of tail of the first household is more variable, observed through distinct letter values, implying that their not-so-regular behavior is quite extreme. This shows, how looking at the distribution of the dependent variable can throw more light on the energy behavior of the customers, which are lost using aggregate or summary statistics.

gravitas R package (Gupta et al. 2019) is used to facilitate the systematic exploration here. While trying to explore the energy behavior of these customers systematically across cyclic time granularities, the first thing we should have at our disposal is to know which all cyclic time granularities we can look at exhaustively. If we consider conventional time deconstructions for a Gregorian calendar (second, minute, half-hour, hour, day, week, fortnight, month, quarter, semester, year), the following time granularities can be considered for this analysis.

```
#> 30m

#> [1] "hhour_hour"      "hhour_day"      "hhour_week"
#> [4] "hhour_fortnight" "hhour_month"     "hhour_quarter"
#> [7] "hhour_semester"  "hhour_year"     "hour_day"
#> [10] "hour_week"       "hour_fortnight" "hour_month"
```

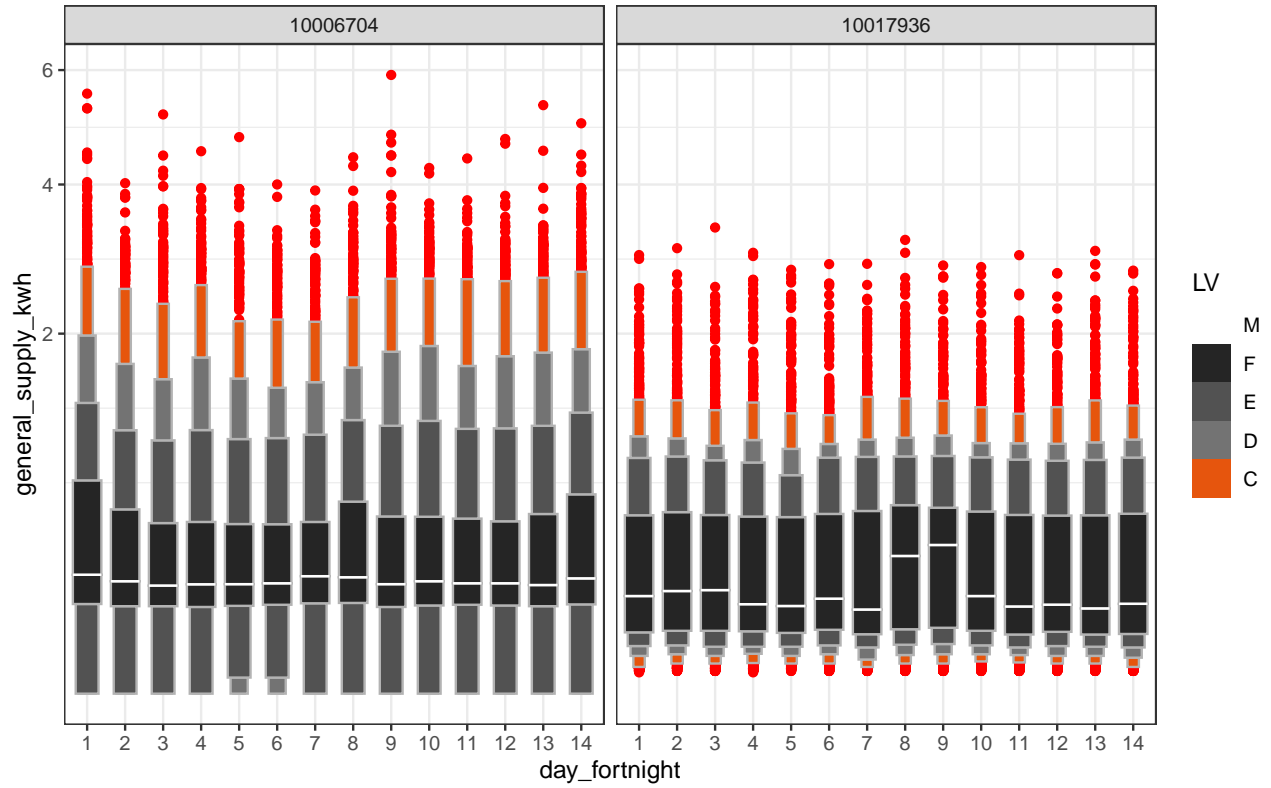


Figure 8: Letter value plot of two households across days of the fortnight. M, F, E, D and C represents the letter values of energy consumption. Regular behavior (within letter value F) is more variable for the 2nd household, whereas extreme behavior (beyond letter value F) is varying more for the first household.

```
#> [13] "hour_quarter"      "hour_semester"      "hour_year"
#> [16] "day_week"          "day_fortnight"      "day_month"
#> [19] "day_quarter"        "day_semester"        "day_year"
#> [22] "week_fortnight"     "week_month"          "week_quarter"
#> [25] "week_semester"      "week_year"           "fortnight_month"
#> [28] "fortnight_quarter"  "fortnight_semester"  "fortnight_year"
#> [31] "month_quarter"      "month_semester"      "month_year"
#> [34] "quarter_semester"   "quarter_year"        "semester_year"
```

The interval of this tibble is 30 minutes, and hence the temporal granularities range from half-hour to year. If these options are considered too many, the most coarse temporal unit can be set to be a “month”.

```
#> [1] "hhour_hour"      "hhour_day"          "hhour_week"
#> [4] "hhour_fortnight" "hhour_month"         "hour_day"
#> [7] "hour_week"        "hour_fortnight"     "hour_month"
#> [10] "day_week"         "day_fortnight"      "day_month"
#> [13] "week_fortnight"   "week_month"         "fortnight_month"
```

Also, some intermediate temporal units that might not be pertinent to the analysis can be removed from the list of cyclic granularities we want to look at.

```
#> [1] "hour_day"      "hour_week"      "hour_month" "day_week"      "day_month"
#> [6] "week_month"
```

Now that we have the list of cyclic granularities to look at, we can visualize the distribution. From the search list, we found six cyclic granularities for which we would like to derive insights of energy behavior. The distribution of energy needs to be visualized across two cyclic granularities at a time. It is equivalent to taking 2 granularities from 6, which essentially is equivalent to visualizing 30 plots. However, harmony/clash pairs can be identified among those 30 pairs, to determine feasibility of plotting any pairs together. We are left with 13 harmonies pair, each of which can be plotted together to look at the energy behavior from different perspectives.

```
smart_meter10 %>% harmony(
  ugran = "month",
  filter_out = c("hhour", "fortnight")
)
```

```
#> # A tibble: 13 x 4
#>   facet_variable x_variable facet_levels x_levels
#>   <chr>          <chr>          <int>    <int>
#> 1 day_week      hour_day           7        24
#> 2 day_month     hour_day          31        24
#> 3 week_month    hour_day           5        24
#> 4 day_month     hour_week          31       168
#> 5 week_month    hour_week           5       168
#> 6 day_week      hour_month         7       744
#> 7 hour_day      day_week           24         7
#> 8 day_month     day_week           31         7
#> 9 week_month    day_week           5         7
#> 10 hour_day     day_month          24        31
#> 11 day_week     day_month           7        31
#> 12 hour_day     week_month          24         5
#> 13 day_week     week_month           7         5
```

```
smart_meter10 %>% gran_advice("wknd_wday", "hour_day")
```

```
#> The chosen granularities are harmonies
#>
```

```

#> Recommended plots are: violin lv quantile boxplot
#>
#> Number of observations are homogenous across facets
#>
#> Number of observations are homogenous within facets
#>
#> Cross tabulation of granularities :
#>
#> # A tibble: 24 x 3
#>   hour_day Weekday Weekend
#>   <fct>      <dbl>    <dbl>
#> 1 0        7705      3097
#> 2 1        7698      3100
#> 3 2        7698      3101
#> 4 3        7698      3102
#> 5 4        7699      3099
#> 6 5        7701      3098
#> 7 6        7700      3099
#> 8 7        7700      3098
#> 9 8        7695      3098
#> 10 9       7696      3098
#> # ... with 14 more rows

```

In Figure 9 we visualize the harmony pair (wknd_wday, hour_day) through a box plot. Boxplot of energy consumption is shown across wknd_wday (facet) and hour-day (x-axis) for the same two households. For the second household, outliers are less prominent implying their regular behavior is more stable. For the first household, energy behavior is not significantly different between weekdays and weekends. For the second household, median energy consumption for the early morning hours is extremely high for weekends compared to weekdays.

For the second household, outliers are less prominent implying their regular behavior is more stable. For the first household, energy behavior is not significantly different between weekdays and weekends. For the second household, median energy consumption for the early morning hours is extremely high for weekends compared to weekdays.

Now, we would like to see how these customers' behavior relate to the rest of the 50 households across these two measures -

- if energy distribution is skewed towards extreme?
- if the weekend and weekday behavior are different for most of these households?

Figure 10 shows the quantile plot of energy consumption of 50 households. Similar quantiles for weekend and weekdays indicate that behaviors of most of these customers do not alter between weekdays and weekends.

Figure 11 shows that the median is very close to the lower boundaries of all the other bands implying energy consumption for these households are left skewed. Moreover, only the pink band changes significantly in winter months (May - August). The median consumption or width of other bands doesn't vary much across seasons, implying extreme behavior or extreme customers does not vary across seasons much. Most of the behavioral changes occur in the quartiles, that too in peak hours of the day. It is to be noted here that the level of quantiles increased too in winter months (obvious because of weather conditions), the interesting part is to notice that the relationship between bands other than quartile stayed same across seasons.

This case study shows systematic exploration of energy behavior starting with two households and comparing some of their features with all 50 households. First, it helps us to find the list of granularities to look at, then shrinks the number of possible visualizations by identifying harmonies and then explored harmony pairs to gain some insights on periodic behavior of the households.

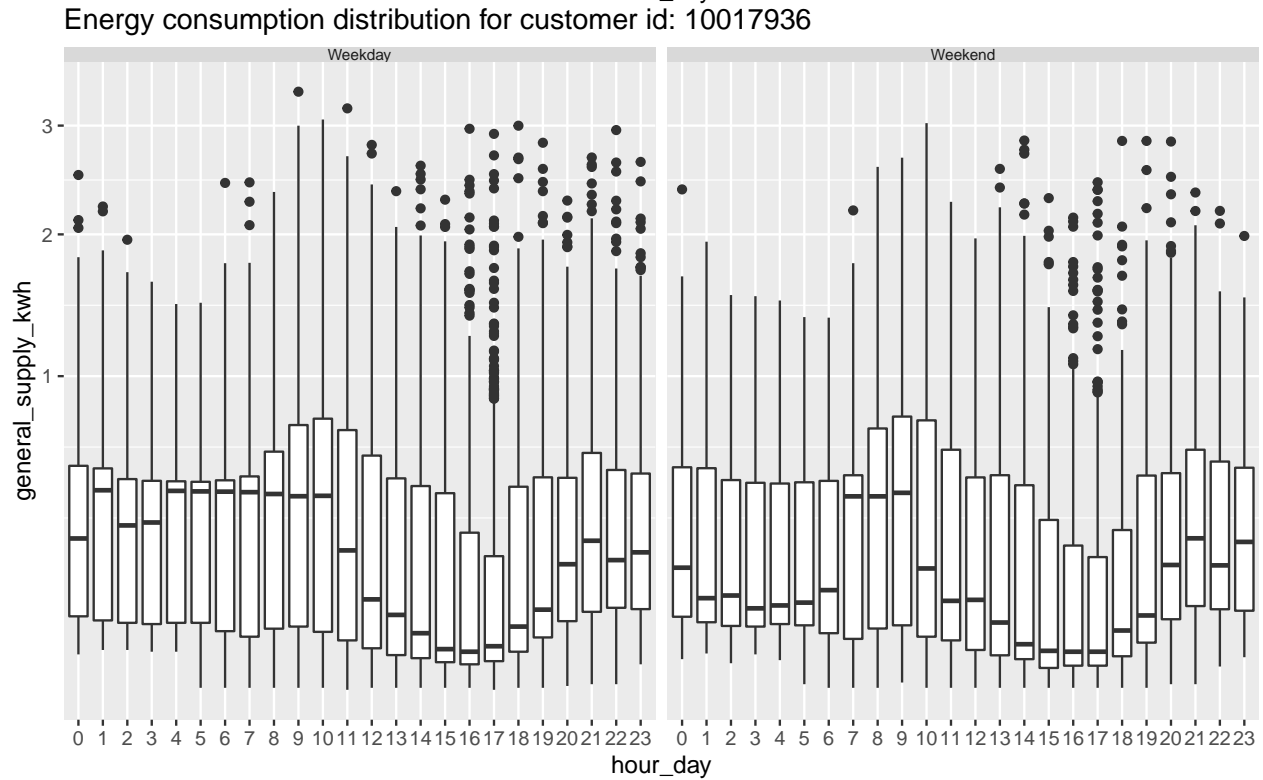
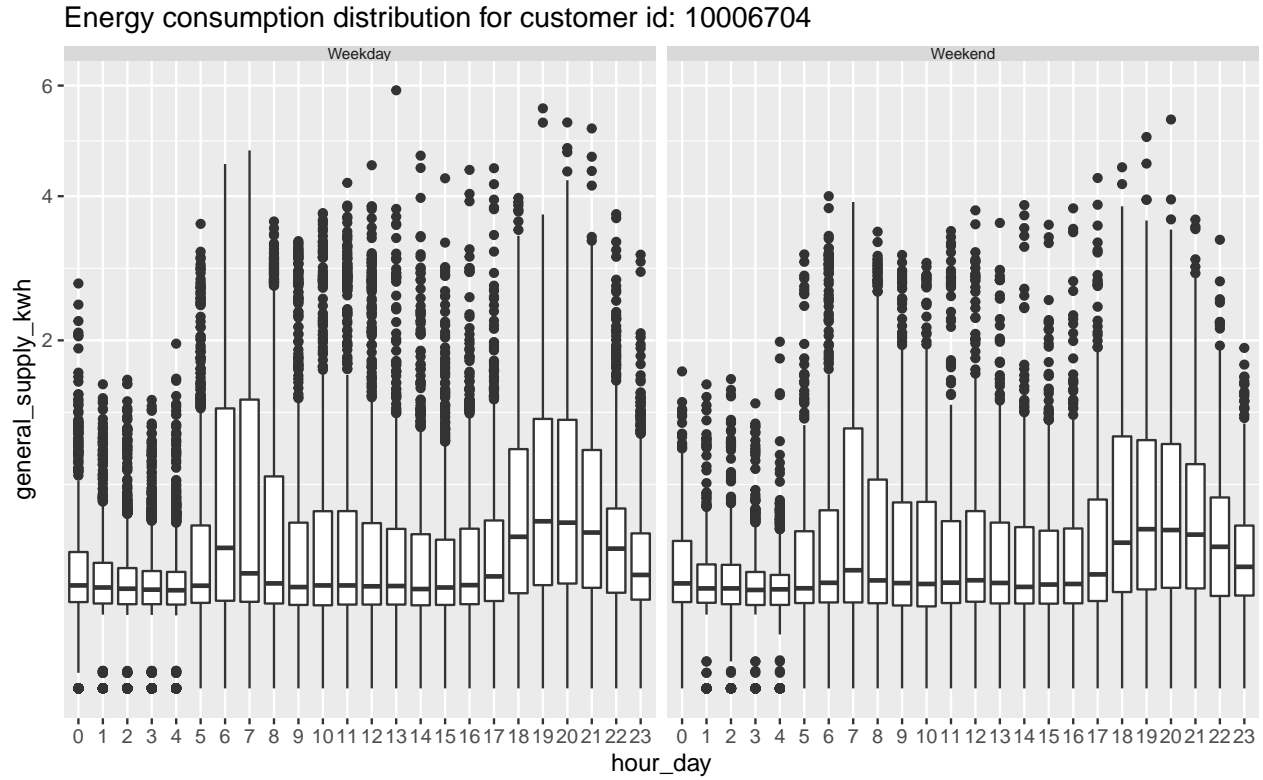


Figure 9: Boxplot of energy consumption across hours of the day faceted by weekday/weekend for household 1 (customer id: 10006704) and household 2 (customer id: 10017936). Median behavior for the early morning hours of household 2 is extremely high for weekends compared to weekdays, not much difference can be observed for household 1.

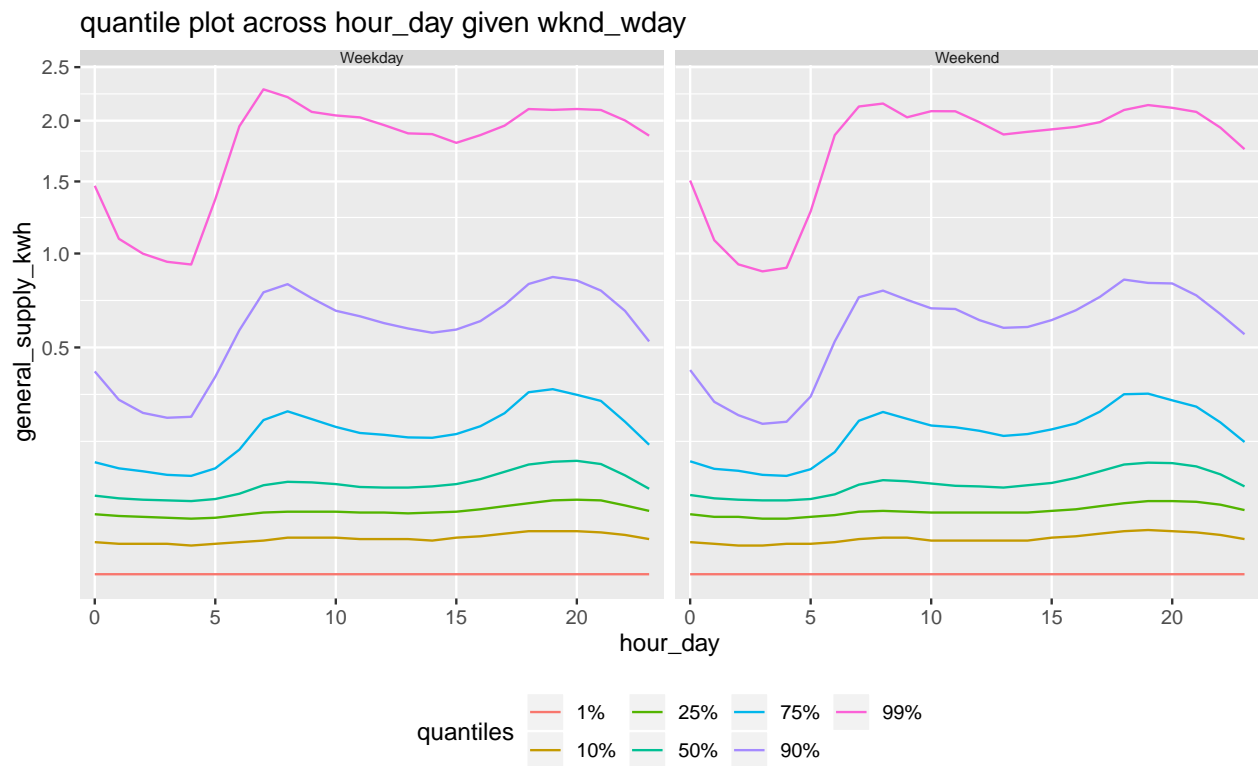


Figure 10: Quantile plot of energy consumption of 50 households across different hours of the day faceted by weekday and weekend. The quantiles are not different for weekdays and weekends implying either the behavior balances out among these customers or most of them do not behave differently for weekdays and weekends.

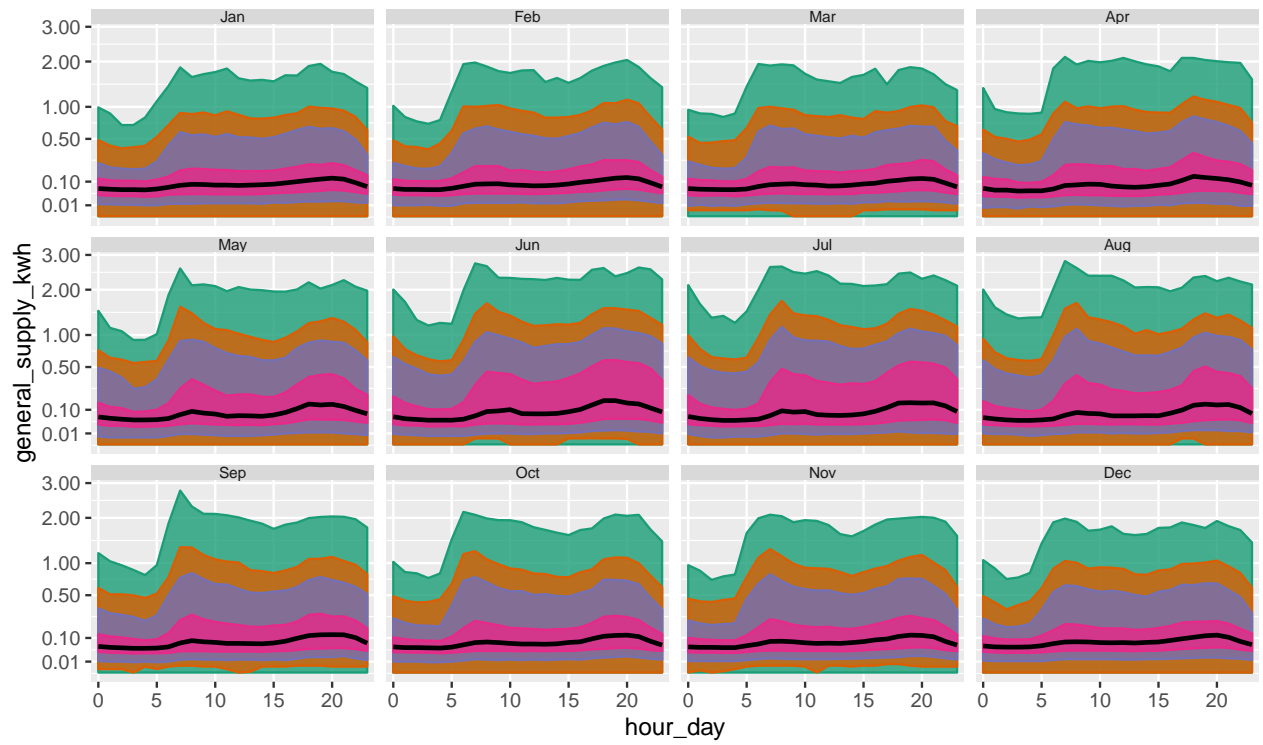


Figure 11: Area quantile plots of energy consumption across hours of the day faceted by months of the year. The black line is the median, whereas the pink band covers 25th to 75th percentile, the orange band covers 10th to 90th percentile and the green band covers 1st to 99th percentile. The median and quartile consumption increase in winter months, but extreme behavior represented by higher bands mostly stay the same across seasons.

7.2 T20 cricket data of Indian Premiere League

The application is not only restricted to temporal data. We provide an example of cricket to illustrate how this can be generalized in other applications. The Indian Premier League (IPL) is a professional Twenty20 cricket league in India contested by eight teams representing eight different cities in India. With eight teams, each team plays each other twice in a home-and-away round-robin format in the league phase. In a Twenty20 game the two teams have a single innings each, which is restricted to a maximum of 20 overs. Hence, in this format of cricket, a match will consist of 2 innings, an innings will consist of 20 overs, an over will consist of 6 balls with some exceptions.

The ball by ball data for IPL season 2008 to 2016 is fetched from Kaggle. The `cricket` data set in the `gravitas` package summarizes the ball-by-ball data cross overs and contains information for a sample of 214 matches spanning 9 seasons (2008 to 2016).

Although there is no conventional time granularity in cricket, we can still represent the data set `cricket` through a `tsibble`, where each over, which represents an ordering from past to future, can form the index of the `tsibble`. The hierarchy table would look like the following:

G	k
over	20
inning	2
match	1

There are many interesting questions that can possibly be answered with such a data set, however, we will explore a few and understand how the proposed approach in the paper can help answer some of the questions.

First, we look at the distribution of runs per over across over of the innings and seasons in Figure 12. The distribution of runs per over has not significantly changed from 2008 to 2016. There is no clear pattern/trend that runs per over is increasing or decreasing across seasons. Hence, we work with subsets of seasons to answer some of the questions:

Q1: How run rates vary depending on if a team bats first or second?

Mumbai Indians(MI) and Chennai Super kings(CSK) are considered one of the best teams in IPL with multiple winning titles and always appearing in final 4 from 2010 to 2015. It would be interesting to take their example in order to dive deeper into the first question.

From Figure 13, it can be observed that there is no clear upward shift in runs in the second innings as compared to the first innings. The variability of runs also increases as the teams approach towards the end of the innings, as observed through the longer and more distinct letter values.

Q2: Is run rate set to reduce in subsequent over if fielding/bowling is good in the previous over? Between fielding and bowling which penalizes runs in the subsequent over more?

For establishing that the fielder fielded well in a particular over, we can see how many catches and run outs were made in that particular over. If a batsman is bowled out, it does not necessarily signify good fielding. So we only include catches and run out as a measure of fielding. Difference in runs across over should be negative if good fielding has an impact on the runs scored in the subsequent overs. Let us see if this fact is true. Figure 14 shows the difference between run rate between two subsequent overs are negative when good fielding leads to one or two dismissals in an over, implying good fielding in one over has indeed an impact on runs scored in the subsequent overs.

```
#> # A tibble: 4 x 21
#>   fielding_wckts  `1`  `2`  `3`  `4`  `5`  `6`  `7`  `8`  `9`
#>   <fct>         <dbl> <dbl> <dbl> <dbl> <dbl> <dbl> <dbl> <dbl> <dbl>
#> 1 0           1039  997  972  978  962  957 1002 1012  993
#> 2 1           120  145  171  165  180  181  138  124  140
```

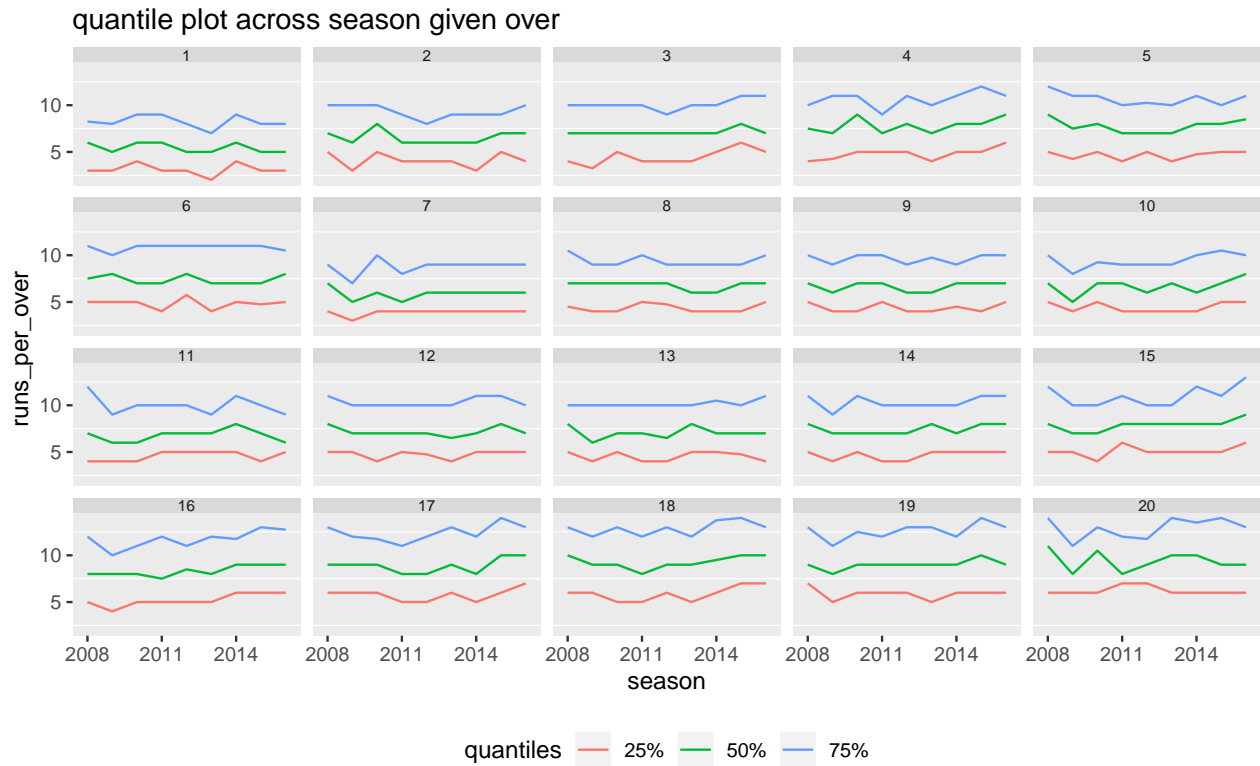


Figure 12: Quantile plot of runs per over across overs of different seasons. There is no pattern on increase or decrease of runs across overs for seasons.

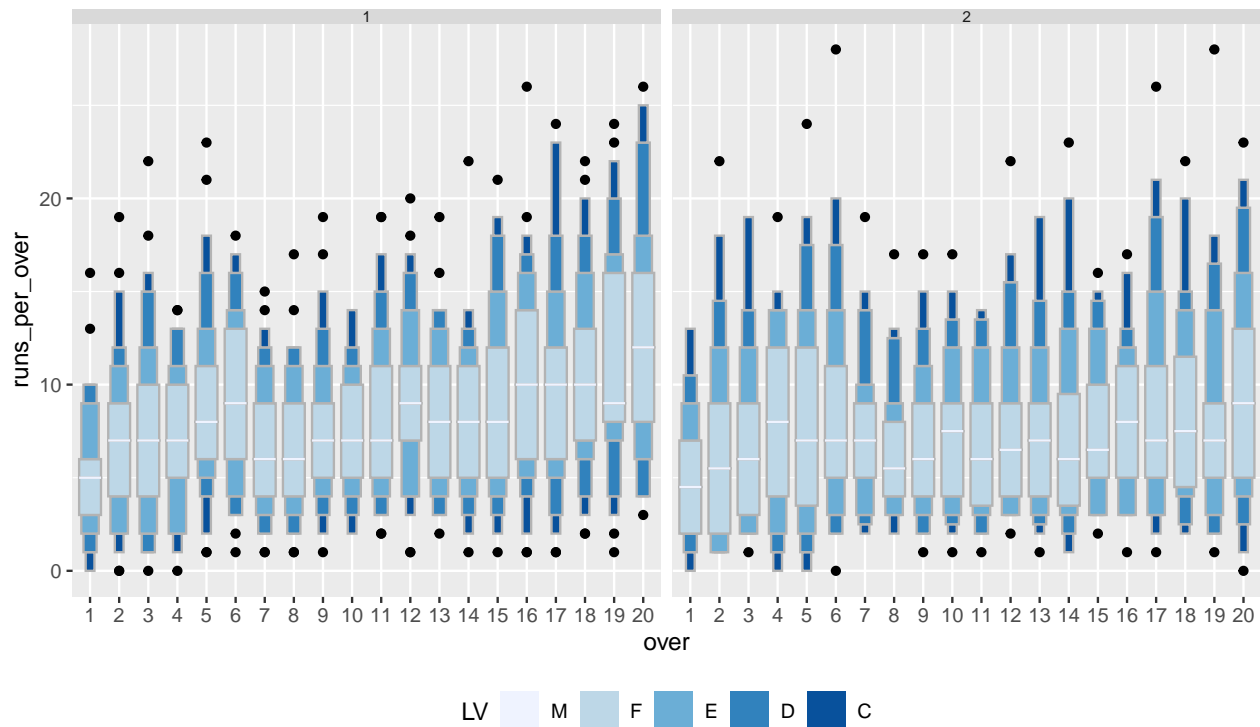


Figure 13: Letter value plot of runs per over across overs of the inning faceted by innings of the match. No upward shift in runs in the second innings like that in the first implying teams are more vulnerable to score more in the first innings as they approach the end of the inning.

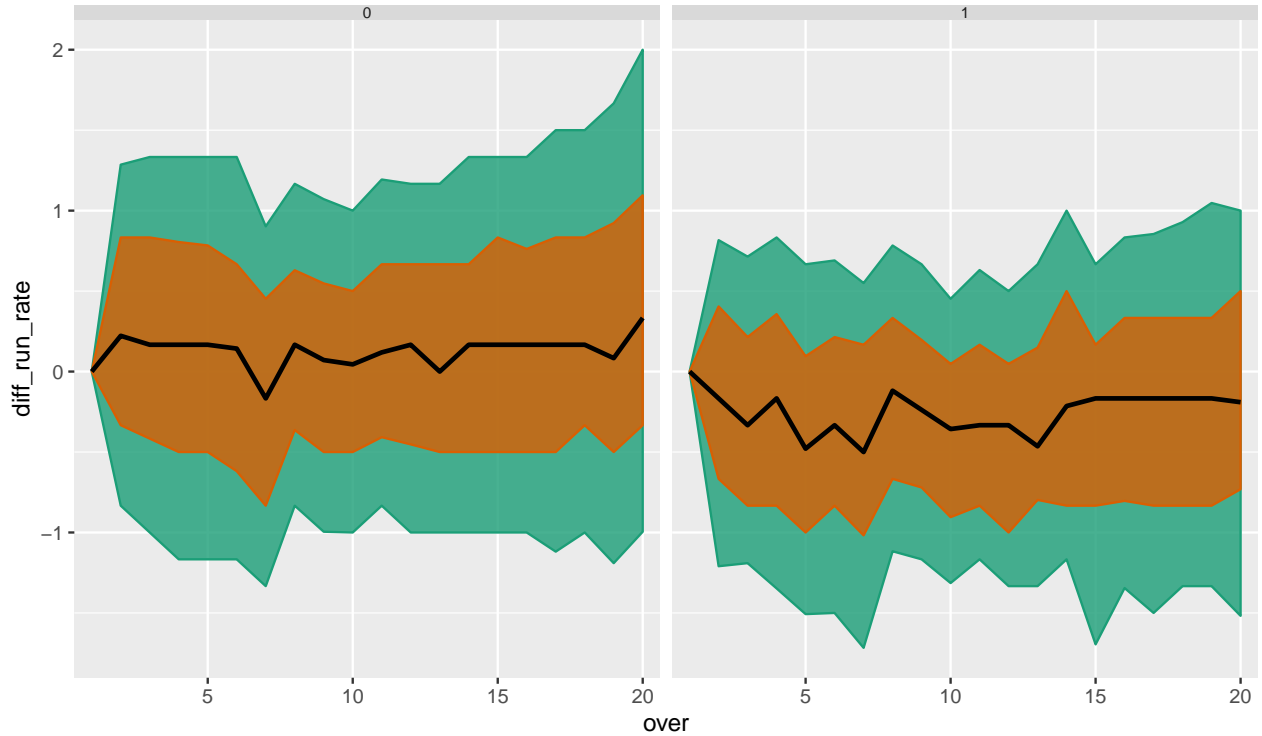


Figure 14: Distribution of lagged run rate across overs of the innings and dismissals by catch and catch and bowled. This shows good fielding in one over leads to lower runs in the subsequent overs for at least 50 percentiles of times.

```
#> 3 2          5    10    8    8    9    10    6    10    8
#> 4 3          0     0    0    0    0     0    0     0    0
#> # ... with 11 more variables: `10` <dbl>, `11` <dbl>, `12` <dbl>,
#> #   `13` <dbl>, `14` <dbl>, `15` <dbl>, `16` <dbl>, `17` <dbl>,
#> #   `18` <dbl>, `19` <dbl>, `20` <dbl>
```

Q3: Is runs set to reduce in the next over for dot balls in this over?

A dot ball is a delivery bowled without any runs scored off it. The number of dot balls is reflective of the quality of bowling in the game. Run rate of an over should ideally decrease if the number of dot balls increase. However, what is the effect of dot balls on runs scored in the subsequent over. Will players batsman likely to go for big shots because they couldn't score good runs in the previous over? Or they should play consistently and avoid scoring high? From figure 15 shows the quantile plot of runs across overs for none, one or two dot balls per over in the facets. Each of the quantiles decrease across facets. With two dot balls per over, at least 50% of the times, run rates decrease in the subsequent over as observed through the negative values for 10th, 25th and 50th percentile quantiles.

8 Discussion

Acknowledgements

9 Bibliography

->

Aigner, Wolfgang, Silvia Miksch, Heidrun Schumann, and Christian Tominski. 2011. *Visualization of*

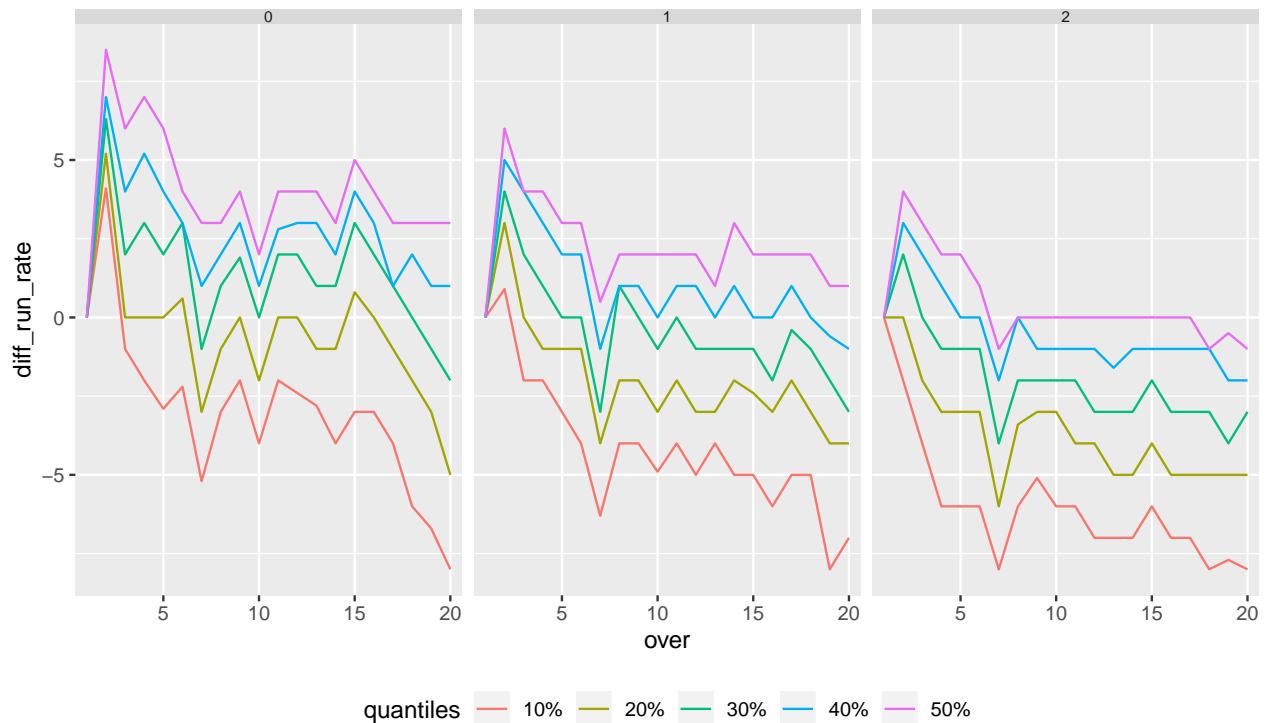


Figure 15: 10th, 20th, 30th, 40th and 50th quantiles of runs per over are drawn across overs of the innings with no (facet 1), one (facet 2) and two (facet 3) dot balls per over. For all three cases, difference in runs between subsequent overs decrease.

Time-Oriented Data. Springer Science & Business Media.

Bettini, Claudio, and Roberto De Sibi. 2000. "Symbolic Representation of User-Defined Time Granularities." *Ann. Math. Artif. Intell.* 30 (1): 53–92.

Bettini, Claudio, Curtis E Dyreson, William S Evans, Richard T Snodgrass, and X Sean Wang. 1998. "A Glossary of Time Granularity Concepts." In *Temporal Databases: Research and Practice*, edited by Opher Etzion, Sushil Jajodia, and Suryanarayana Sripada, 406–13. Berlin, Heidelberg: Springer Berlin Heidelberg.

Department of the Environment and Energy. 2018. *Smart-Grid Smart-City Customer Trial Data*. Australian Government, Department of the Environment; Energy: Department of the Environment; Energy, Australia. <https://data.gov.au/dataset/4e21dea3-9b87-4610-94c7-15a8a77907ef>.

G Grolemond, H Wickham. 2011. "Dates and Times Made Easy with Lubridate." *Journal of Statistical Software*.

Goodwin, S And Dykes, 2012. "Visualising Variations in Household Energy Consumption." *IEEE Conference on Visual Analytics Science and Technology (VAST)*.

Gupta, Sayani, Rob Hyndman, Di Cook, and Antony Unwin. 2019. *Gravitas: Explore Probability Distributions for Bivariate Temporal Granularities*. <https://CRAN.R-project.org/package=gravitas>.

Hintze, Jerry L, and Ray D Nelson. 1998. "Violin Plots: A Box Plot-Density Trace Synergism." *Am. Stat.* 52 (2). [American Statistical Association, Taylor & Francis, Ltd.]: 181–84.

Hofmann, Heike, Hadley Wickham, and Karen Kafadar. 2017. "Letter-Value Plots: Boxplots for Large Data." *J. Comput. Graph. Stat.* 26 (3). Taylor & Francis: 469–77.

Hyndman, Rob J. 1996. "Computing and Graphing Highest Density Regions." *Am. Stat.* 50 (2). [American Statistical Association, Taylor & Francis, Ltd.]: 120–26.

- Mcgill, Robert, John W Tukey, and Wayne A Larsen. 1978. “Variations of Box Plots.” *Am. Stat.* 32 (1). Taylor & Francis: 12–16.
- Ning, Peng, Xiaoyang Sean Wang, and Sushil Jajodia. 2002. “An Algebraic Representation of Calendars.” *Ann. Math. Artif. Intell.* 36 (1): 5–38.
- Potter, K, J Kniss, R Riesenfeld, and C R Johnson. 2010. “Visualizing Summary Statistics and Uncertainty.” *Comput. Graph. Forum* 29 (3): 823–32.
- Reingold, Edward M, and Nachum Dershowitz. 2001. *Calendrical Calculations Millennium Edition*. Cambridge University Press.
- Tukey, John W. 1977. *Exploratory Data Analysis*. Vol. 2. Reading, Mass.
- Wang, Earo, Dianne Cook, and Rob J Hyndman. 2018. “Calendar-Based Graphics for Visualizing People’s Daily Schedules.”
- . 2019. “A New Tidy Data Structure to Support Exploration and Modeling of Temporal Data.” *Journal of Computational and Graphical Statistics*. <https://doi.org/10.1080/10618600.2019.1695624>.
- Wickham, Hadley. 2016. *Ggplot2: Elegant Graphics for Data Analysis*. Springer-Verlag New York. <http://ggplot2.org>.
- Wilkinson, Leland. 1999. *The Grammar of Graphics*.